Memory reactivation of real-world spatial orientation revealed by human electrophysiology.

Thomas Schreiner[1], Benjamin J. Griffiths[1,2], Merve Kutlu[1], Christian Vollmar[3], Elisabeth Kaufmann[3], Stefanie Quach[4], Jan Remi[3], Soheyl Noachtar[3] & Tobias Staudigl[1]

1. Department of Psychology, Ludwig-Maximilians-Universität München, Germany.
2. Centre for Human Brain Health, University of Birmingham, United Kingdom.
3. Epilepsy Center, Department of Neurology, Ludwig-Maximilians-Universität München, Germany.
4. Department of Neurosurgery, University Hospital Munich, Ludwig-Maximilians-Universität München, Germany

Abstract

Spatial navigation and memory are thought to rely on common neuronal mechanisms, enabling us to travel in physical and mental space. Seminal findings in animal models support this assumption. However, how navigation and memory processes interact in humans is not well understood. Here we tested whether real-world head orientations act as spatial context for memories by investigating their reactivation during wake and sleep. We recorded intracranial electrophysiology in epilepsy patients and scalp EEG in healthy participants while they retrieved real-world head orientations as well as while targeted memory reactivation (TMR) was applied during subsequent non-rapid eye movement (NREM) sleep. We show that head orientation-related signals are reactivated during successful memory retrieval, suggesting that they provide specific memories with spatial information. Moreover, we found that TMR triggered reactivation of prior learned head orientations during sleep. Sleep related memory reactivation was paralleled and predicted by increased power in the SO-spindle range while being accompanied by elevated levels of ripples recorded intracranially from the medial temporal lobe. In conclusion, our results suggest that core features of spatial navigation add contextual spatial information to newly formed memory traces.

Introduction

Spatial navigation and memory are assumed to rely on common neuronal mechanisms, enabling us to travel in physical and mental space [1]. Consequentially, basic types of navigation are thought to map onto separate memory systems [2]: Path integration, enabling spatial navigation based on self-motion cues without the need for landmarks, is thought to share neural mechanisms with episodic memory, the system that enables us to remember autobiographical events in a spatio-temporal context [3]. Both path integration and episodic memory are self-referenced, meaning that their reference-frames rest within the agent that either navigates an environment or remembers personal events. While essential neural features of path integration have been characterized on a neural level in rodents navigating physical space [4], their counterparts in humans navigating memory space are less well described.

A fundamental requirement to any type of navigation is a sense of orientation. Animal models identified head direction cells as essential for the neural manifestation of a sense of orientation [5]. These cells fire when the animal is oriented in a particular direction with respect to the environment [6]. By indicating an animal's directional heading, they act as a "neural compass" during spatial navigation [7]. While these spatially tuned cells are comparatively well studied in rodents [8], we are only beginning to understand the neural basis of the human sense of direction [9,76]. In particular, when it comes to incorporating real-world features of navigation that comprise self-motion, many human studies face challenges because they rely on fixed head and body positions (e.g., fMRI, MEG). Restricting self-motion will, however, prevent the generation of self-motion cues which are thought to be fundamental for studying the neural basis of navigation [10,11].

Here we set out to investigate the mnemonic function of real-world spatial orientations and asked what role spatial orientation could play in human memory. In spatial navigation, heading orientation can be used to disambiguate locations that share common features, such as identical distances from the origin. Indeed, disturbing the head direction system in rodents renders spatial information ambiguous and impairs both the mapping of the environment [12–14] and navigation behavior [7]. In memory, spatial orientation could thus be used as what is commonly called a memory context, adding cues to a memory trace. These cues could be used to disambiguate similar memory traces. Hence, during the encoding of novel events, information about the current head orientation could be stored alongside to-be-remembered information, providing contextual information. We tested the relevance of real-world head orientation for memory by investigating memory reactivation during wake and sleep. Given the essential role of reactivation processes for episodic memory retrieval and the consolidation of memories during sleep [15], relevant orientation-related signals are expected to emerge during the retrieval of corresponding memory traces as well as during sleep.

To investigate how head orientation serves memory, we recorded scalp EEG in healthy participants and intracranial electrophysiology in epilepsy patients while they retrieved real-world spatial memories (i.e., prior learned head orientation – image associations). Importantly, head orientations were linked to specific sound cues, which were presented again during

subsequent non-rapid eye movement (NREM) sleep to trigger the reactivation of head orientation related representations (i.e., targeted memory reactivation, TMR [16]). We find that head orientation-related electrophysiological signatures are reactivated during successful awake memory retrieval as well as during TMR while participants were asleep, suggesting that spatial information is stored alongside episodic memories. During sleep, memory reactivation was predicted by increased power in the SO-spindle range while being accompanied by elevated levels of medial temporal lobe (MTL) ripples, illustrating the importance of sleep oscillations for the re-processing of real-world spatial memories [17].

Results [EEG – healthy participants]

Twenty-five participants (age: 25.2 ± 0.6; 16 female) took part in the EEG study. Experimental sessions started in the evening around 7 p.m. After an initial training phase (see Methods), participants performed a real-world spatial memory task, where they learned to associate 168 items (images of objects) with specific head orientations (see Fig. 1a). Importantly, a specific sound cue was assigned to each of the four head orientations. After a delay filled with a distractor task, memory performance was tested in a stepwise manner. First, participants made object-recognition judgments (old or new). Then, for recognized images only, participants indicated which of the four head orientations was associated with the item during the learning phase (associative memory test, Fig. 1a). After finishing the memory task, participants went to sleep. During NREM sleep, 2 out of the 4 sounds (one sound associated with the right-sided and one with the left-sided head orientations, respectively) were repeatedly presented as TMR cues, while an additional sound, unrelated to the learning, served as a control sound. We reasoned that presenting TMR cues during sleep would ignite reactivation of the related head orientations and the associated items.

Behavioral results

To test for potential differences in memory performance between test times and TMR conditions, we conducted an ANOVA for the cued recall, including the factors cueing (cued vs. uncued) and test-time (pre- vs. post- sleep). Results indicated that memory performance declined over the course of sleep (main factor test-time: $F_{1,24} = 19.24$; $p < 0.001$). Importantly though, the interaction between test-time and cueing ($F_{1,24} = 5.48$; $p = 0.028$) was also significant, indicating that TMR did modulate memory performance. However, TMR did not benefit memory performance as expected [18] but had a detrimental effect on retrieval abilities (cued pre-sleep: 57.23 ± 3.92% vs. cued post-sleep: 50.42 ± 4.56%; uncued pre-sleep: 58.76 ± 4.13% vs. uncued post-sleep: 54.90 ± 4.61%; see Fig. 1b). For recognition memory we neither found a significant main effect of test time ($F_{1,24} = 0.29$; $p = 0.59$); nor a significant interaction between test-time and cueing ($F_{1,24} = 0.08$; $p = 0.77$; see Supplementary Fig. 1 for details).

Head orientations are reactivated during successful retrieval.

Next, we set out to test whether we could decode remembered head orientations from EEG signals during retrieval, which (i) would provide evidence that head orientations enrich memory

traces with spatial context and (ii) would allow us to track corresponding reactivation processes during TMR (see below). To extract the head orientation-related patterns of neuronal activity during retrieval, we pooled the associative retrieval data (i.e., when participants had to remember image related head orientations) across pre- and post-sleep sessions. Furthermore, we restricted the analysis to correctly remembered head orientations that were selected for TMR (i.e., one left sided and one right sided head orientation per participant) and performed multivariate classification (linear discriminant analysis; LDA) on these data (Fig. 1c +d). Using fivefold cross-validation (see Methods), above-chance classification accuracy emerged around the onset of the associative retrieval prompt (peak at 270 ms; $p < 0.001$, corrected for multiple comparisons across time). Hence, the retrieval data allowed us to isolate brain patterns associated with the reactivation of remembered head orientations, which we then used to guide the analysis of memory reactivation during TMR (for results concerning the classification of later uncued head orientations during retrieval see Supplementary Fig. 2).

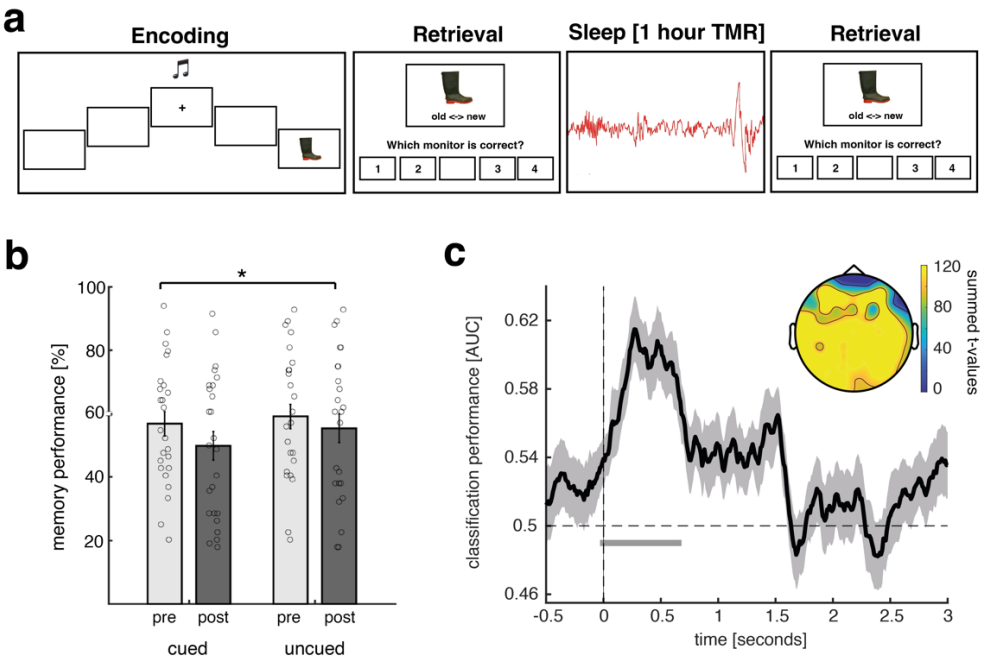

Fig. 1 Experimental procedure, behavioral results, and retrieval locked reactivation of head orientations. (a) During encoding, participants were presented with 168 images (EEG study) / 144 images (iEEG study) of objects on four flanking screens (positioned at -60°, -30°, +30° and 60° relative to the center screen). Before, one of four animal sounds was played, predicting the relevant orientation. During NREM sleep, two of the learning-related sounds (one related to left-sided and one related to right-sided orientation) and one control sound, were presented again for 60 minutes. Memory performance was tested before and after a night of sleep in a stepwise manner. First, participants made object-recognition judgments (old or new). Then, for recognized images only, participants indicated which of the four head orientations was associated with the item during the learning phase (b) Behavioral results for both experimental sessions pre- (light gray) and post-sleep (dark gray), separated into cued and uncued trials. Bar graphs show mean (±SEM) percentage of recalled head orientations. Dots indicate individual memory performance of participants (N = 25). Stars denote significant differences as derived from a repeated measures ANOVA ($F_{1,24} = 5.48$; $p = 0.028$). (c) Later cued head orientations (left vs. right) could be reliably decoded (above chance) from the retrieval data, starting around the onset of the associate prompt (the black solid line indicates decoding performance (±SEM)). The horizontal dashed line indicates chance level performance (i.e., 0.5). The vertical solid line indicates the onset of associative memory test trials (time = 0). The lower horizontal gray line shows the temporal extent of significant decoding results as derived from a dependent-samples t-test (two-sided, $p < 0.001$, cluster corrected across time). The topographical insert illustrates the results of a "searchlight decoding procedure", indicating that bilateral centro-parietal and occipital areas exhibited stimulus-category related effects (please note that statistical tests were done for illustrative purposes only).

TMR ignites reactivation of head orientation representations during NREM sleep.

First, we tested whether TMR induced electrophysiological activity would discriminate between learning related and control sounds. Consistent with previous findings [19–21], the direct comparison (see Fig. 2a) revealed that learned TMR cues, as compared to control cues, triggered a significant increase in power in the SO-spindle range (i.e., an initial low frequency burst followed by a fast spindle burst; $p < 0.001$, corrected for multiple comparisons across time, frequency, and space), foreshadowing that learning-related TMR cues might have triggered relevant neuronal processing in the sleeping brain.

To specifically test this notion, we next determined whether neuronal activity related to remembered head orientations would be reactivated during TMR. We first trained a classifier on the concatenated retrieval data from both pre- and post-sleep sessions [−0.5 to 1s]. The resulting training weights were then applied on the TMR data [-0.5 to 1.5 s]. Classifier testing labels reflected the stimulus categories used in the retrieval sessions (left- or right-sided head orientation), such that above-chance classification hallmarks TMR related activation patterns more strongly resembling the related stimulus category than the alternative stimulus category. As shown in Fig. 2b, results revealed significant above-chance classification from 930 to 1410 ms relative to TMR onset ($p = 0.023$, corrected for multiple comparisons across time; retrieval time-window [-110 to 330 ms]), emerging during the presence of sleep spindles. Applying the decoding procedure to source-space data, revealed that these effects might have originated from fronto-parietal networks and the right medial temporal lobe (including the entorhinal cortex, the parahippocampus and the hippocampus; see Fig. 2c).

Finally, we asked whether the oscillatory fingerprint of TMR in the SO-spindle range (Fig. 2a) would be instrumental for TMR triggered memory reactivation to unfold. To address this question, we correlated, across participants, TMR triggered power (averaged across the cluster shown in Fig. 2a) and levels of mean classification performance (averaged across the cluster shown in Fig. 2b). As shown in Fig. 2d, we observed a significant positive relationship between the two variables (rho = 0.50, $p = 0.01$; for classification results based on TMR trials exhibiting increased levels of activity in the SO-spindle range see Supplementary Fig. 3).

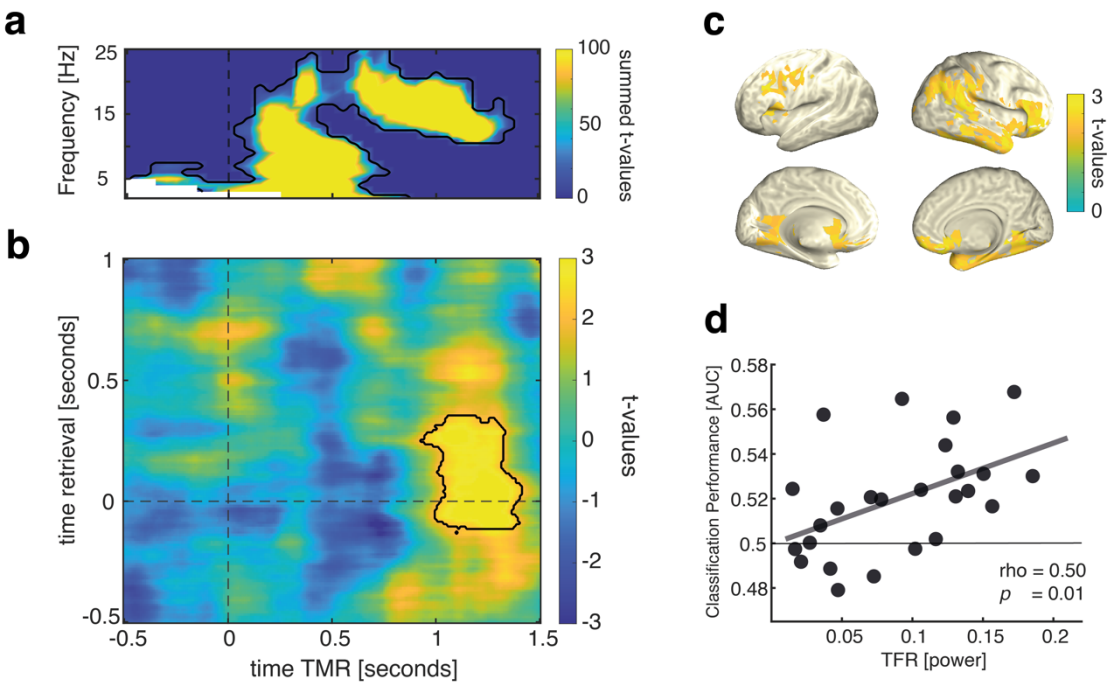

Fig. 2 Reactivation of head orientation representations during TMR. (a) Power difference between learning-related TMR cues versus new control cues after statistical thresholding ($p < 0.001$, corrected) (b) Learning-related brain patterns (left vs. right head orientations) were decodable during TMR (contour lines indicate the extent of the cluster, $p = 0.023$ corrected; color range (blue to yellow) represents t values against chance level performance. (c) The source plots illustrate the results of a "searchlight decoding procedure", indicating that fronto-parietal networks and the right medial temporal lobe exhibited head orientation related effects (please note that statistical tests were done for illustrative purposes only). (d) classification performance correlated positively with TMR triggered power (r = 0.50, $p = 0.01$).

Results [intracranial EEG - patients]

Ten patients took part in the intracranial EEG (iEEG) study. Overall, the procedures of the experiment were highly similar to the above-described scalp EEG study but optimized for patients in a clinical setting (e.g., reduced trial number in the memory task, memory task was split into consecutive blocks etc.; for details see Methods).

Behavioral results

First, we tested whether the effects of TMR on memory performance, as reported above, would replicate in the patient sample. Hence, we again tested for differences in memory performance between test times and TMR conditions by conducting an ANOVA for the cued recall (factors: cueing (cued vs. uncued) and test-time (pre- vs. post- sleep)). Results revealed that patients' memory performance also declined over the course of sleep (main factor test-time: $F_{1,9} = 32.0$; $p < 0.001$), comparable to the healthy participants' decline. As in the healthy sample, we found a significant interaction between test-time and cueing ($F_{1,9} = 8.28$; $p = 0.018$), indicating that TMR did modulate memory performance by exerting a detrimental effect on retrieval abilities (cued pre-sleep: 58.47 ± 6.02% vs. cued post-sleep: 42.36 ± 4.89%; uncued pre-sleep: 58.88 ± 5.60% vs. uncued post-sleep: 49.58 ± 5.73%; see Fig. 3a). For recognition memory, there was neither a significant main effect of test time ($F_{1,9} = 0.06$; $p = 0.08$); nor a significant interaction between test-time and cueing ($F_{1,9} = 2.25$; $p = 0.16$; see Supplementary Fig. 4 for details).

Head orientation representations are reactivated during successful retrieval.

Next, we assessed whether the intracranial data would reveal evidence for the reactivation of remembered head orientations during retrieval, in line with the results of the EEG study. Again, the associative retrieval data was pooled across pre- and post-sleep sessions, and multivariate classification (LDA) was restricted to correctly remembered items where the associated head orientations were cued during sleep (i.e., one left sided and one right sided head orientation per patient). Using fivefold cross-validation (see Methods), significant above-chance classification accuracy emerged after the onset of the associative retrieval prompt (peak at 200 ms; $p = 0.014$, corrected for multiple comparisons across time). Hence, similar to scalp EEG recordings, multivariate classification during retrieval using iEEG activity allowed us to isolate brain patterns associated with the reactivation of remembered head orientations.

TMR trigged reactivation of head-orientation representations is accompanied by ripple activity.

In a first step we tested again whether TMR triggered power would distinguish between learning related and control sounds. In line with the results of the scalp EEG study, learned TMR cues, as compared to control cues, elicited a significant power increase in in the SO-spindle range in frontal and parietal contacts (low frequency cluster: $p < 0.001$; spindle cluster: $p < 0.001$; corrected for multiple comparisons across time and frequency, Fig. 3c). Next, we determined whether TMR-triggered reactivation of head orientation representations would be traceable in the intracranial data. A classifier was trained on the concatenated retrieval data from both pre- and post-sleep sessions [−0.5 to 1s] and the resulting training weights were applied on the TMR data [-0.5 to 1.5 s]. Given the clear association between power in the SO-spindle range and classification performance in the scalp EEG study (see Fig. 2d), we confined the analysis on TMR trials exhibiting increased power in the SO-spindle range (see Methods for details; see Supplementary Fig. 5 for a direct comparison between high and low power trials). We found a cluster of significant above-chance classification from 760 to 1270 ms relative to TMR onset ($p = 0.004$, corrected for multiple comparisons across time, retrieval time-window [-180 to 100 ms]; Fig. 3d), indicating the reactivation of remembered head orientations during the presence of cortical spindles.

In contemporary models of memory consolidation, hippocampal ripples have been closely linked to reactivation of previous learning experiences and in consequence the memory function of sleep [22,23]. Hence, we tested whether there would be any temporal relationship between the presence of MTL ripples and the obtained reactivation metrics. We extracted ripples in the medial temporal lobe (7 patients, 14 contacts) based on established criteria [24] (see Methods for details; see Fig. 3e). To investigate the timing of MTL ripples (centered at the maximal negative amplitude) with regards to TMR cues, we created peri-event histograms (bin size = 50 ms) of ripple events time-locked to TMR cues. As shown in Fig. 3d (black inset) ripple density exhibited a clear peak when remembered head orientations were decodable from the intracranial recordings and spindles were present in cortical leads. To quantify the relationship between ripple density and the reactivation signal, we averaged the classification output

across the relevant retrieval time [-180 to 100 ms] and correlated the patient-averaged classification output with the patient-averaged ripple density across time. We found a significant positive relationship between the classification performance and ripple density (rho = 0.41, p = 0.007; see Fig. 3f; also see Supplementary Fig. 6) indicating the functional relevance of ripples for memory reactivation.

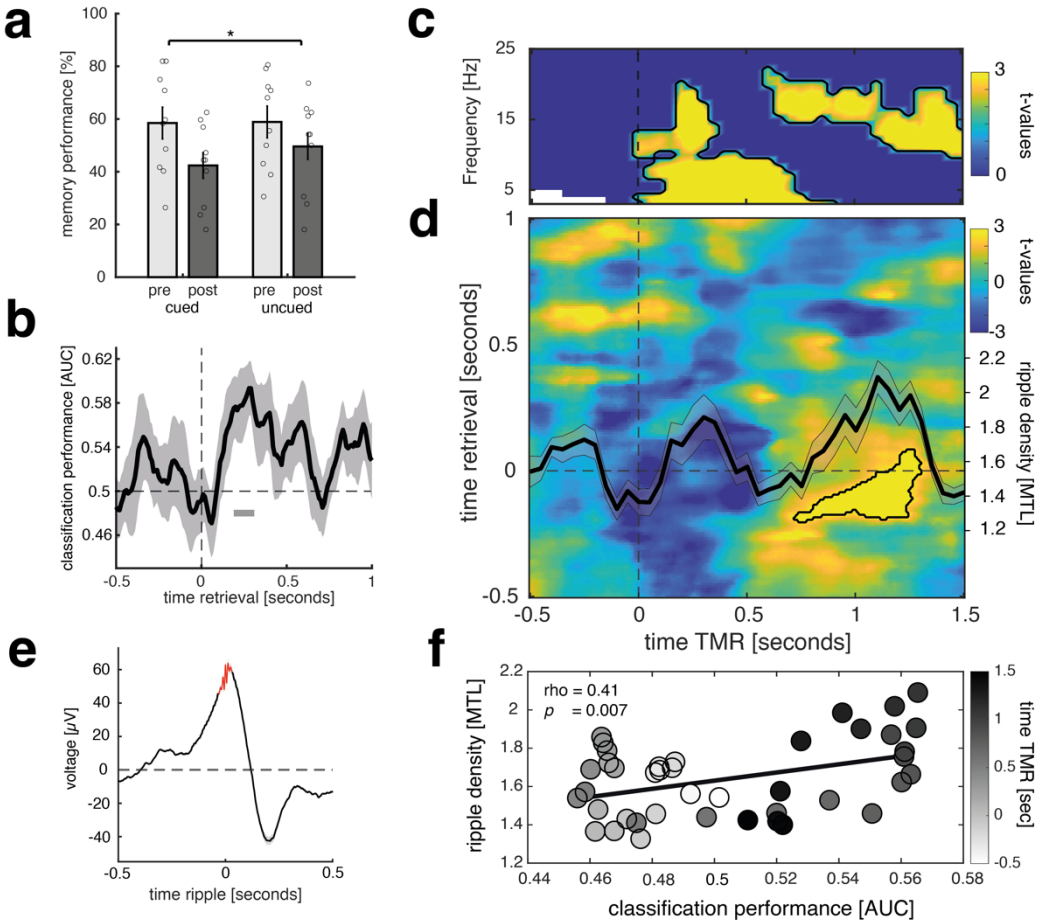

Fig.3 iEEG study. (a) Behavioral results for both experimental sessions pre- (light gray) and post-sleep (dark gray), separated into cued and uncued trials. Bar graphs show mean (±SEM) percentage of recalled head orientations. Dots indicate individual memory performance of participants (N = 10). Stars denote significant differences as derived from a repeated measures ANOVA ($F_{1,9}$ = 8.28; p = 0.018). (b) Later cued head orientation (left vs. right) could be reliably decoded (above chance) from the retrieval data, starting around 190 ms after the onset of the associate prompt (the black solid line indicates decoding performance (±SEM)). The horizontal dashed line indicates chance level performance (i.e., 0.5). The vertical solid line indicates the onset of associative memory test trials (time = 0). The lower horizontal gray line shows the temporal extent of significant decoding results as derived from a dependent-samples t-test (two-sided, p = 0.014, cluster corrected across time). (c) Power difference indicating that learning-related TMR cues triggered increased power in frontal and parietal contacts (p < 0.05, corrected) as compared to control cues. (d) Head orientation-related brain patterns (left vs. right) were decodable during TMR (contour lines indicate the extent of the cluster, p = 0.004 corrected; color range (blue to yellow) represents t values against chance level performance. The black line illustrates the density of MTL derived ripples (bin size = 50 ms; 7 patients, 14 contacts) across TMR trials. (e) grand average of all detected ripples (7 patients, 14 contacts; locked to maximal negative amplitude) during 'high power' TMR trials (66.57 ± 10.57 ripples in 119.07 ± 7.27 trials). (f) The classification output (Fig. 3d), averaged across retrieval time [-180 to 100 ms] and patients, correlated positively with the patient-averaged ripple density across TMR time (TMR time color coded, with white corresponding to data segment onset (-0.5 s) and black corresponding to the end of segments (1.5 s; rho = 0.41, p = 0.007).

Discussion

Our results demonstrate that head orientation-related signals are reactivated both during successful memory retrieval while wake and TMR during sleep, suggesting that they provide memory-relevant contextual spatial information alongside specific item memories. Moreover, we found that TMR-triggered reactivation of remembered head orientations was accompanied by elevated levels of MTL ripples and increased SO-spindle power, illustrating the importance of sleep oscillations for the re-processing of real-world spatial memories.

Based on seminal findings in animal models, it has been proposed that spatial navigation and memory rely on common neuronal mechanisms [2], involving the same core brain structures [25]. However, whether this also holds for humans and to what extend navigation and memory related processes directly interact is unclear. Here, we asked whether real-world head orientation serves a memory function, by investigating their reactivation during retrieval and sleep. Our results speak for this notion, by showing that the reactivation of head orientation-related signatures is detectable both during successful memory retrieval during wake and TMR during sleep, and thus provide evidence that head orientation signals might enrich memory traces with spatial context in humans.

The finding that TMR triggered memory reactivation of contextual head orientation representations is accompanied by elevated levels of MTL ripples, nicely corresponds with the commonly ascribed role of ripples in memory consolidation: mediating memory reactivation during sleep [22,23,26]. While to date, evidence for a role of ripples in facilitating memory reactivation during sleep in humans has been scarce, ripples have been closely associated with reactivation of prior experiences in rodents [22]. Interestingly, hippocampal ripples have also been shown to be tightly linked to head orientation signals during sleep in rodents [27]. Even though the authors did not specifically assess memory reactivation in their study, their results align with our data demonstrating that head orientation signals might provide ripple related memory reactivation with spatial information. However, while the ripple mediated reactivation of information is thought to represent the prime vehicle of systems consolidation, sleep's cardinal oscillations (SOs and spindles) and their interplay have since long been assumed to play a crucial role in this context [28–33]. Namely, by relaying the reactivated information between the hippocampus and neocortical long-term stores [22,23,34]. Our finding that reactivation processes were paralleled and predicted by increased power in the SO-spindle range further corroborates the necessity of sleep oscillations for memory consolidation [35–37]. In sum, we demonstrate the importance of sleep oscillations for memory reactivation to unfold and provide evidence that ripples might be intimately related to TMR triggered re-processing of memories during sleep.

As already mentioned, we used TMR as an experimental tool to trigger contextual memory reactivation during sleep. It has been consistently shown that TMR efficiently modulates memory capabilities and leads most often to a strengthening of performance [18,38–42]. Considering these findings, our result that TMR did not benefit but deteriorate memory performance in healthy participants, which we replicated in patients, might seem surprising.

However, a growing number of studies reported TMR impairments, when several targets (in our case images) were associated with a given TMR cue / context (in our case sounds / head orientations) [20,43,44]. It has been suggested that if cue-target pairs differ in their memory strength, TMR might specifically elicit reactivation of the strongest representations, due to competition between pairs [43]. While we did not explicitly manipulate memory strength, our results seem to be in line with this interpretation, given that the strength of the association between cues and targets might have varied substantially in our data (note that 42 images were associated with each sound/ head orientation in the scalp EEG study; 36 in the iEEG study). Furthermore, participants were not encouraged to integrate memories together, which has been shown to promote benefits in case of multi-target TMR [21,45]. Finally, in an exploratory analysis (see Supplementary Fig. 7) we find that the identification of TMR elicited memory reactivation might have mainly relied on high confidence retrieval trials, potentially suggesting that stable memory traces outcompeted weaker ones in their rivalry for being reactvated by a TMR cue.

Ultimately, our results might speak for the notion that spatial orientation could be used as what is commonly called a memory context, hence adding cues to specific memory traces. It is well known that human episodic memory is highly context dependent [46,47]. When an experience is retrieved in the same context as it was encoded, memory performance is higher as compared to when it is remembered in a different context [48, but see 49]. Contexts also influence how information is retrieved, as retrieving a memory that occurred in a particular real-world location leads to the spontaneous retrieval of other memories that shared the same spatial context [50]. Similar effects have also been shown for temporal [51] (i.e., memories formed within temporal proximity of others) and sematic [52] (i.e., memories sharing semantic relatedness) contexts. Moreover, prior encoded spatial and non-spatial contextual information is reactivated during retrieval [53–56] and sleep [57]. Our findings extend these previous results by showing that real-world contextual information provided by veridical head orientations are stored alongside specific item memories given that they are reactivated during successful retrieval and during sleep, when prompted by TMR.

In conclusion, we used invasive and non-invasive human electrophysiology to reveal memory reactivation of real-world head orientation during wake and sleep. Our results suggest that head orientation signals act as contextual cues in episodic memory, akin to their functional role in spatial navigation. While these findings provide unique insights into how spatial navigation and episodic memory intersect on a neural level, future work will need to carve out further functional overlaps between episodic memory processes and navigation mechanisms.

Methods

Participants

25 healthy, right-handed participants (mean age: 25.2 ± 0.6; 16 female) with normal or corrected-to-normal vision took part in the EEG experiment. An additional 14 participants had to be excluded due to insufficient sleep or technical problems. The sample size was determined in accordance with previous human sleep and memory studies (e.g., [35,58,59]). Pre-study screening questionnaires (including the Pittsburgh Sleep Quality Index (PSQI [60]), the morningness–eveningness questionnaire [61], and a self-developed questionnaire querying general health status and the use of stimulants) indicated that participants did not take any medication at the time of the experimental session and did not suffer from any neurological or psychiatric disorders. All participants reported good overall sleep quality. Furthermore, they had not been on a night shift for at least 8 weeks before the experiment. All participants were instructed to wake up by 7 a.m. and avoid alcohol the evening before and caffeine on the day of the experimental sessions. They received course credit or financial reimbursement in return for their participation. All participants gave written informed consent after being informed about the details of the study. The study was approved by the ethics committee of the Department of Psychology (Ludwig–Maximilian Universität Munich).

For the iEEG study, 10 patients from the Epilepsy Center, Department of Neurology, Ludwig–Maximilian Universität (Munich, Germany), all suffering from medically intractable epilepsy, volunteered. An additional four patients had to be excluded due to technical difficulties. The study was approved by the ethics committee of the Medical Faculty of the Ludwig–Maximilian Universität.

Stimuli and procedures

Overview. On experimental days participants arrived at the sleep laboratory at 7 p.m. The experimental session started with the set-up for polysomnographic recordings during which electrodes for electroencephalographic (EEG) and electrooculography (EOG) were applied. Several days prior to the experimental session, participants were habituated to the environment by having an adaptation nap in the sleep laboratory. At around 8 p.m. the experiment started with a training task, followed by the memory task (for details see Training and Memory Task below). The sleep period began at ~11 p.m. and all participants slept for ~7 h (for sleep characteristics see Supplementary Tables 1). During NREM sleep (sleep stages N2 and SWS), some of the animal sounds, which were presented before during the training and the memory task were presented again for 60 minutes (see Targeted memory reactivation for details). Participants were awoken after 6 to 7 hours of sleep from light sleep (sleep stage N1 or N2) and after 15 min of recovery and memory performance was tested again.

For the iEEG study the general approach was largely similar. Experimental procedures were arranged around the clinical routines. Specifically, the training sessions were executed during daytime, while the memory task was employed after dinner (i.e., starting between ~6-7 pm).

Patients went to sleep between 10 and 12 p.m. and slept for ~7 h (for sleep characteristics see Supplementary Tables 2). As with the EEG study, animal sounds were presented for 60 minutes during NREM sleep. Post-sleep memory performance was tested the next morning.

Stimuli. A set of in total 336 images of objects and five animal sounds (i.e., a cow's moo, a parrot's squawk, a cat's meow, a sheep's baa, a cuckoo's sound) served as experimental stimuli. Objects were images of animals, food, clothing, tools, or household items presented on a plain white back- ground. All images were taken from [62].

Experimental tasks. For the recording of behavioral responses and the presentation of all experimental tasks, Psychophysics Toolbox Version 3 [63] and MATLAB 2018b (MathWorks, Natick, USA) were used. Responses were made via keyboard presses on a dedicated PC. Across all experimental phases, presentation order of stimuli was randomized across participants / patients.

Training. Participants / patients began by fixating on the center screen, where a fixation cross was presented for 1.5 ± 0.1 seconds. The cross disappeared and one of four animal sounds was played (600 ms). Subsequently, the cross appeared on one of four flanking screens (positioned at -60°, -30°, +30° and 60° relative to the center screen, duration: 2.5 seconds, see Fig. 1a). Four of the total five sounds were randomly chosen at the start of the experiment and randomly assigned to a single flanking screen. The assignment of sound to screen remained fixed across the whole experiment. Participants / patients were instructed to turn their head to face the screen which the fixation cross appeared on and maintain fixation upon the cross (duration: 2.5 seconds). Afterwards, the fixation cross re-appeared on the center screen for 1.5 (± 0.1) seconds and participants had to bring their head back to the starting (i.e., central) position. The training session consisted of 160 trials, split across 4 blocks (i.e., 40 trials per block). The aim of the session was enabling participants / patients to form strong and stable associations between the sound cues and the corresponding head orientations (i.e., flanking screens).

Memory task [EEG study]. Participants in the EEG study learned to associate 168 images of objects with specific head orientations. Each trial started with a fixation cross, presented for 1.5 ± 0.1 seconds. Afterwards, one of the four animal sounds from the training phase was played (duration 600ms). Subsequently, an image of an object was presented on the corresponding flanking screen for 4 seconds (the assignment of sound to screen was known to the participants from the training). Participants were instructed to turn their head to face the screen which the image appeared on and to remember the images and their position. Afterwards, the participants had to indicate via button press whether the previously seen object was animate or inanimate, with the question being presented on the center screen. The pre-sleep memory test included the 168 images from encoding (old items) intermixed with 84 new images, which were not seen by the participants before ("foils"). Each trial started with a

fixation cross, presented for 1.5 ± 0.1 s. After the fixation cross, an image was presented on the center screen. After 1 second, participants were asked to indicate whether the image was "old" (i.e., part of the learning material) or "new"' (i.e., it was not seen during learning) within the next 10 s. In case of "new" responses, participants immediately moved on to the next trial. In case of "old" responses, participants were required to indicate by button press the related head orientation (i.e., the flanking screen on which the image was presented). Each trial ended with participants indicating how confident they were with their head orientation decision (scale from 0 corresponding to very uncertain to 4, very certain). The post-sleep retrieval followed the same procedures as the pre-sleep memory test with the exception that new foil images were used.

Memory task [iEEG study]. The procedures of the memory task were similar to the EEG study, with some modifications. The stimulus pool was comprised of 288 objects (drawn from the same selection as used in the EEG study). In order not to overtax patients, the pre-sleep memory task was split into three consecutive encoding - retrieval blocks. During each encoding block patients were presented with 48 images on the flanking screens (please note that the trial level was identical to the one described above). Each encoding block was followed by a retrieval block, where the 48 images from encoding intermixed with 24 new images were presented. Hence, across all blocks, we used 144 images as old items and 72 images as new items. As above, patients had to first indicate whether a given image was old or new and in case of old items specify the remembered head orientation. Due to time constraints no confidence rating was obtained. The post-sleep retrieval was executed in one run, meaning that patients were confronted with the 144 images which were part of the learning material and 72 foils.

Targeted memory reactivation. For targeted memory reactivation 2 out of the 4 sounds presented during training and encoding were selected. Specifically, we randomly picked one out of the two sounds associated with the left-sided head orientations (i.e., flanking screens positioned at -60° and -30°) and one sound associated with the right-sided head orientations (i.e., flanking screens positioned at 30° and 60°). In addition, the fifth animal sound which was not used during training and encoding served as a control stimulus. The three cues were repeatedly presented during NREM sleep via loudspeaker with an intertrial interval of 5.5 ± 0.2 seconds (~50 dB sound pressure level) for a maximum of 60 minutes (EEG study: 182.6 ± 31.41 repetitions per stimulus; iEEG study: 187.1 ± 23.7 repetitions per stimulus). Sound presentation was stopped whenever signs of arousals, awakenings or REM sleep became visible.

Scalp EEG acquisition. An EEGo 65 channel EEG system (ANT Neuro Enschede, Netherlands) was used to record electro- encephalography (EEG) throughout the experiment. Impedances were kept below 20 kΩ. EEG signals were referenced online to electrode CPz and sampled at a rate of 1000 Hz. Furthermore, horizontal and vertical EOG was recorded for

polysomnography. Sleep architecture was determined offline according to standard criteria by two independent raters [64].

iEEG acquisition. Intracranial EEG was recorded from Spencer depth electrodes (Ad-Tech Medical Instrument, Racine, Wisconsin, United States) with 4–12 contacts each, 5 mm apart. Data were recorded using XLTEK Neuroworks software (Natus Medical, San Carlos, California, US) and an XLTEK EMU128FS amplifier, with voltages referenced to a parietal electrode site. The sampling rate was set at 1,000 Hz.

EEG data analysis. EEG data were preprocessed using the FieldTrip toolbox for EEG/MEG analysis [65]. All data were down-sampled to 200 Hz. Subsequently, the pre- and post-sleep retrieval as well as the TMR data were segmented into epochs. For the retrieval data we focused our analyses on time windows when participants had to deliberately remember the prior associated head orientation, as memory reactivation of associated head orientation representations should be particularly strong here due to the potential hippocampal dependency (as compared to recognition testing [66]). Hence, we segmented the retrieval data around the question prompt with regards to the image related head orientations. The temporal range of the epochs was [–1 to 3 s] around stimulus onset for retrieval and TMR trials. Noisy EEG channels were identified by visual inspection, discarded, and interpolated, using a weighted average of the neighboring channels. The data were visually inspected and artefactual trials were removed. The retrieval data were additionally subjected to an independent component analysis (ICA) and ICA components associated with eye blinks and eye movements were identified and rejected.

iEEG data analysis. The preprocessing steps for the iEEG data were identical to the ones described above, just that iEEG data were additionally inspected for epileptic activity, with data segments comprising epileptic events at any given channel being discarded. In addition, contacts which were contaminated with epileptiform background activity were discarded. Only seizure-free nights were included in the analysis.

Source level. To estimate the sources of the obtained effects in the scalp EEG study, we applied a DICS beamforming method [67], as implemented in FieldTrip [65]. A spatial filter for each specified location (each grid point; $10mm^3$ grid) was computed based on the cross -spectral density, calculated separately for all retrieval and TMR trials. Electrode locations for the 65-channel EEGo EEG system were co-registered to the surface of a standard MRI template in MNI (Montreal Neurological Institute) space using the nasion and the left and right preauricular as fiducial landmarks. A standard leadfield was computed using the standard boundary element model [68]. The forward model was created using a common dipole grid (10mm3 grid) of the grey matter volume (derived from the anatomical automatic labeling atlas [69] in MNI space, warped onto standard MRI template, leading to 1457 virtual sensors. Data analysis was accomplished in the same way as on sensor level.

Time–frequency analysis. Time–frequency analysis of the TMR segments (memory related and control cues) was performed using FieldTrip. Frequency decomposition of the data, using Fourier analysis based on sliding time windows (moving forward in 50 ms increments). The window length was set to five cycles of a given frequency (frequency range: 1–25 Hz in 1 Hz steps). The windowed data segments were multiplied with a Hanning taper before Fourier analysis. Afterwards, power values were z-scored across time [−1 to 3 s]. The longer time segments were chosen to allow for resolving low frequency activity within the time windows of interest [−0.5 to 1.5 s] and avoid edge artifacts.

Multivariate analysis. Multivariate classification of single-trial EEG data was performed using MVPA-Light, a MATLAB-based toolbox for multivariate pattern analysis [70]. For all multivariate analyses, a LDA was used as a classifier. Prior to classification, data in both studies were re-referenced using a common average reference (CAR).

For classification within the retrieval task, the localizer data were z-scored across all trials for each time point separately. Next, data from the pre- and the post-sleep retrieval were collapsed and subjected to a principal component analysis (PCA), which transforms the data into linearly uncorrelated components, ordered by the amount of variance explained by each component [71]. PCA was applied to reduce dimensionality and limit over-fitting (PCA) and the first 30 principal components were retained for further analysis. To quantify whether representations of prior learned head orientations can be differentiated during retrieval, the classifier was trained and tested to discriminate between the later cued head orientations (i.e., one left sided and one right sided head orientation; see Targeted Memory reactivation for details). Only trials belonging to remembered head orientations entered the analysis. Data were smoothed using a running average window of 150 ms. The EEG channels / iEEG contacts served as features and a different classifier was trained and tested on every time point. As metric, we used Area Under the ROC Curve (AUC), which indexes the mean accuracy with which a randomly chosen pair of Class A and Class B trials could be assigned to their correct classes (0.5 = random performance; 1.0 = perfect performance). To avoid overfitting, data were split into training and test sets using fivefold cross- validation [72]. Since cross-validation results are stochastic due to the random assignment of trials into folds, the analysis was repeated five times and results were averaged. For statistical evaluation, the classification output was tested against chance levels (i.e., 0.5). To resolve the topography of diagnostic features in the scalp EEG data, we conducted a "searchlight decoding procedure" (Fig. 2 c). In brief, PCA components were projected back to sensor space and the classification procedure was repeated across moving kernels of small electrode clusters, with neighboring electrodes being selected as features [feature number range: 5 to 9]. Finally, classification values were collapsed across our time windows of interest [retrieval time: -30 to 680 ms;] and tested against chance level (corrected for multiple comparisons across space).

To investigate whether TMR would elicit head orientation related representations, we used the temporal generalization method [73]. Prior to decoding, a baseline correction was applied based on the whole trial for retrieval and TMR segments [−0.5 to 3 s]. Next, retrieval and TMR

data were z-scored across trials and collapsed. PCA was applied to the pooled retrieval-TMR data and the first 30 principal components were retained. Retrieval and TMR data were smoothed using a running average window of 150 ms. A classifier was then trained for every time point in the retrieval data and applied on every time point during TMR. No cross-validation was required since retrieval and TMR datasets were independent. As metric, we again used AUC (see above). For statistical evaluation, the classification output was tested against chance levels (i.e., 0.5). Due to the close relationship of power in the SO-spindle range and classification performance (see Fig. 2d) in the EEG study, we focused the multivariate analysis in the iEEG study on TMR trials exhibiting clear SO-spindle characteristics. First, we compared TMR locked power in all frontal and parietal contacts (N = 202) between prior learned TMR cues and control cues (which were not part of the learning material). As in the EEG study, TMR cues elicited stronger activity in the SO-spindle range as compared to control cues (see Fig 3c). Next, for each patient we sorted the TMR trials as a function of power in the before obtained cluster and divided the trials using a median split. To enhance the signal to noise ratio only 'high-power' TMR trials were subjected to the multivariate analysis. For the scalp EEG data, head orientations were decoded in source space using searchlight analysis [74]. A sphere of radius 2 cm was centered on each of the 1467 voxels in the brain. All voxels within the sphere that were inside the brain volume (10-26 voxels) were selected as features. Identical to the sensor level analysis a classifier was trained for every time point in the retrieval data and applied on every time point during TMR. Finally, classification values were collapsed across our time windows of interest [retrieval time: -110 to 330 ms;] and tested against chance level (corrected for multiple comparisons across space).

Ripple detection. Ripple events in the medial temporal lobe (MTL) depth recordings (7 patients, 14 contacts in total: 4 hippocampal, 7 parahippocampal and 3 entorhinal contacts) were detected during artifact-free TMR segments using offline algorithms [24,75]. The iEEG signal was band-pass filtered from 80 to 120 Hz and the root mean square signal (RMS) was calculated based on a 20 ms windows followed by an additional smoothing with the same window length. A ripple event was identified whenever the smoothed RMS-signal exceed a threshold, defined by the mean plus 2 times the standard deviation of the RMS-signal across all TMR data points. Potential ripple events shorter than 25 ms or longer than 300 ms were rejected. All ripple events were required to exhibit a minimum of three cycles in the raw signal.

Peri-event histograms of ripple occurrence. To investigate the timing of MTL ripples (centered at the maximal negative amplitude) with regards to TMR cues, we created peri-event histograms (bin size = 50 ms) of ripple events time-locked to TMR cues. The resulting histograms were normalized by the total number of TMR trials (multiplied by 100).

Statistics. Behavioral retrieval data were subjected to a 2 (TMR: cued/uncued) × 2 (Test-Time: Pre-sleep/Post-sleep) repeated measures ANOVA. The statistical significance thresholds for all behavioral analyses were set at $p < .05$. FieldTrip's cluster permutation test [65] was used to

deal with the multiple comparisons problem for all classification analyses. A dependent-samples t-test was used at the sample level to identify clusters of contiguous time points across participants and values were thresholded at $p = 0.05$. Monte Carlo simulations were used to calculate the cluster p value (alpha = 0.05, two-tailed) under the permutation distribution. Analyses were performed at the group level. The input data were either classification values across time (Fig. 1c + 3b) or time x time classification values (Fig. 2b + 3c). In all cases a two-sided cluster permutation test with 1000 randomizations was used to contrast classification accuracy against chance performance. The same statistical rationale was implemented for the statistical assessment of time frequency data with time × frequency values as input. Statistical analysis of TFR data in the iEEG study was performed at the individual electrode/contact level (fixed-effects analysis), considering all frontal and parietal contacts (N = 202). Pearson correlation was used to assess the relationship between (i) classification performance and time-frequency power (Fig. 2d) and (ii) the time-course of classification performance and ripple density (Fig. 3d).

References

1. Burgess, N., Maguire, E. A. & O'Keefe, J. The human hippocampus and spatial and episodic memory. Neuron 35, 625–641 (2002).
2. Buzsáki, G. & Moser, E. I. Memory, navigation and theta rhythm in the hippocampal-entorhinal system. Nat Neurosci 16, 130–138 (2013).
3. Tulving, E. Elements of Episodic Memory. (Oxford University Press, 1983).
4. McNaughton, B. L., Battaglia, F. P., Jensen, O., Moser, E. I. & Moser, M.-B. Path integration and the neural basis of the 'cognitive map'. Nat Rev Neurosci 7, 663–678 (2006).
5. Taube, J. S. Head direction cells and the neurophysiological basis for a sense of direction. Prog Neurobiol 55, 225–256 (1998).
6. Taube, J. S. The head direction signal: origins and sensory-motor integration. Annu Rev Neurosci 30, 181–207 (2007).
7. Butler, W. N., Smith, K. S., van der Meer, M. A. A. & Taube, J. S. The Head-Direction Signal Plays a Functional Role as a Neural Compass during Navigation. Curr Biol 27, 1259–1267 (2017).
8. Cullen, K. E. & Taube, J. S. Our sense of direction: progress, controversies and challenges. Nat Neurosci 20, 1465–1473 (2017).
9. Jacobs, J., Kahana, M. J., Ekstrom, A. D., Mollison, M. V. & Fried, I. A sense of direction in human entorhinal cortex. Proc Natl Acad Sci U S A 107, 6487–6492 (2010).
10. Steel, A., Robertson, C. E. & Taube, J. S. Current Promises and Limitations of Combined Virtual Reality and Functional Magnetic Resonance Imaging Research in Humans: A Commentary on Huffman and Ekstrom (2019). J Cogn Neurosci 33, 159–166 (2021).
11. Taube, J. S., Valerio, S. & Yoder, R. M. Is navigation in virtual reality with FMRI really navigation? J Cogn Neurosci 25, 1008–1019 (2013).
12. Harland, B. et al. Lesions of the Head Direction Cell System Increase Hippocampal Place Field Repetition. Current Biology 27, 2706-2712.e2 (2017).
13. Calton, J. L. et al. Hippocampal place cell instability after lesions of the head direction cell network. J Neurosci 23, 9719–9731 (2003).
14. Winter, S. S., Clark, B. J. & Taube, J. S. Spatial navigation. Disruption of the head direction cell network impairs the parahippocampal grid cell signal. Science 347, 870–874 (2015).
15. Schreiner, T. & Staudigl, T. Electrophysiological signatures of memory reactivation in humans.

Philos Trans R Soc Lond B Biol Sci 375, 20190293 (2020).
16. Oudiette, D. & Paller, K. A. Upgrading the sleeping brain with targeted memory reactivation. Trends Cogn Sci 17, 142–149 (2013).
17. Navarrete, M., Valderrama, M. & Lewis, P. A. The role of slow-wave sleep rhythms in the cortical-hippocampal loop for memory consolidation. Current Opinion in Behavioral Sciences 32, 102–110 (2020).
18. Hu, X., Cheng, L. Y., Chiu, M. H. & Paller, K. A. Promoting memory consolidation during sleep: A meta-analysis of targeted memory reactivation. Psychol Bull 146, 218–244 (2020).
19. Göldi, M., van Poppel, E. A. M., Rasch, B. & Schreiner, T. Increased neuronal signatures of targeted memory reactivation during slow-wave up states. Sci Rep 9, 2715 (2019).
20. Oyarzún, J. P., Morís, J., Luque, D., Diego-Balaguer, R. de & Fuentemilla, L. Targeted Memory Reactivation during Sleep Adaptively Promotes the Strengthening or Weakening of Overlapping Memories. J. Neurosci. 37, 7748–7758 (2017).
21. Schechtman, E. et al. Multiple memories can be simultaneously reactivated during sleep as effectively as a single memory. Commun Biol 4, 1–13 (2021).
22. Girardeau, G. & Lopes-Dos-Santos, V. Brain neural patterns and the memory function of sleep. Science 374, 560–564 (2021).
23. Klinzing, J. G., Niethard, N. & Born, J. Mechanisms of systems memory consolidation during sleep. Nat Neurosci 22, 1598–1610 (2019).
24. Ngo, H.-V., Fell, J. & Staresina, B. Sleep spindles mediate hippocampal-neocortical coupling during long-duration ripples. eLife 9, e57011 (2020).
25. Squire, L. R. Memory and the hippocampus: a synthesis from findings with rats, monkeys, and humans. Psychol Rev 99, 195–231 (1992).
26. Buzsáki, G. Hippocampal sharp wave-ripple: A cognitive biomarker for episodic memory and planning. Hippocampus 25, 1073–1188 (2015).
27. Viejo, G. & Peyrache, A. Precise coupling of the thalamic head-direction system to hippocampal ripples. Nat Commun 11, 2524 (2020).
28. Sirota, A., Csicsvari, J., Buhl, D. & Buzsáki, G. Communication between neocortex and hippocampus during sleep in rodents. Proc Natl Acad Sci U S A 100, 2065–2069 (2003).
29. Oyanedel, C. N., Durán, E., Niethard, N., Inostroza, M. & Born, J. Temporal associations between sleep slow oscillations, spindles and ripples. Eur J Neurosci 52, 4762–4778 (2020).
30. Staresina, B. P. et al. Hierarchical nesting of slow oscillations, spindles and ripples in the human hippocampus during sleep. Nat Neurosci 18, 1679–1686 (2015).
31. Maingret, N., Girardeau, G., Todorova, R., Goutierre, M. & Zugaro, M. Hippocampo-cortical coupling mediates memory consolidation during sleep. Nat Neurosci 19, 959–964 (2016).
32. Latchoumane, C.-F. V., Ngo, H.-V. V., Born, J. & Shin, H.-S. Thalamic Spindles Promote Memory Formation during Sleep through Triple Phase-Locking of Cortical, Thalamic, and Hippocampal Rhythms. Neuron 95, 424-435.e6 (2017).
33. Helfrich, R. F. et al. Bidirectional prefrontal-hippocampal dynamics organize information transfer during sleep in humans. Nat Commun 10, 3572 (2019).
34. Paller, K. A., Creery, J. D. & Schechtman, E. Memory and Sleep: How Sleep Cognition Can Change the Waking Mind for the Better. Annu Rev Psychol 72, 123–150 (2021).
35. Cairney, S. A., Guttesen, A. Á. V., El Marj, N. & Staresina, B. P. Memory Consolidation Is Linked to Spindle-Mediated Information Processing during Sleep. Curr Biol 28, 948-954.e4 (2018).
36. Schreiner, T., Petzka, M., Staudigl, T. & Staresina, B. P. Endogenous memory reactivation during sleep in humans is clocked by slow oscillation-spindle complexes. Nat Commun 12, 3112 (2021).
37. Abdellahi, M. E. A., Koopman, A. C. M., Treder, M. S. & Lewis, P. A. Targeting targeted memory reactivation: Characteristics of cued reactivation in sleep. NeuroImage 266, 119820 (2023).
38. Schreiner, T. & Rasch, B. Boosting Vocabulary Learning by Verbal Cueing During Sleep. Cereb Cortex 25, 4169–4179 (2015).

39. Schreiner, T., Lehmann, M. & Rasch, B. Auditory feedback blocks memory benefits of cueing during sleep. Nat Commun 6, 8729 (2015).
40. Antony, J. W., Gobel, E. W., O'Hare, J. K., Reber, P. J. & Paller, K. A. Cued memory reactivation during sleep influences skill learning. Nat Neurosci 15, 1114–1116 (2012).
41. Schönauer, M., Geisler, T. & Gais, S. Strengthening procedural memories by reactivation in sleep. J Cogn Neurosci 26, 143–153 (2014).
42. Lewis, P. A. & Bendor, D. How Targeted Memory Reactivation Promotes the Selective Strengthening of Memories in Sleep. Curr Biol 29, R906–R912 (2019).
43. Joensen, B. H. et al. Targeted memory reactivation during sleep can induce forgetting of overlapping memories. Learn Mem 29, 401–411 (2022).
44. Antony, J. W., Cheng, L. Y., Brooks, P. P., Paller, K. A. & Norman, K. A. Competitive learning modulates memory consolidation during sleep. Neurobiology of Learning and Memory 155, 216–230 (2018).
45. Antony, J. W. & Schechtman, E. Reap while you sleep: consolidation of memories differs by how they were sown. Preprint at https://doi.org/10.31234/osf.io/u48fp (2022).
46. Stark, S. M., Reagh, Z. M., Yassa, M. A. & Stark, C. E. L. What's in a context? Cautions, limitations, and potential paths forward. Neuroscience Letters 680, 77–87 (2018).
47. Rudy, J. W. Context representations, context functions, and the parahippocampal-hippocampal system. Learn Mem 16, 573–585 (2009).
48. Tulving, E. & Thomson, D. M. Encoding specificity and retrieval processes in episodic memory. Psychological Review 80, 352–373 (1973).
49. Murre, J. M. J. The Godden and Baddeley (1975) experiment on context-dependent memory on land and underwater: a replication. R Soc Open Sci 8, 200724 (2021).
50. Griffiths, B., Mazaheri, A., Debener, S. & Hanslmayr, S. Brain oscillations track the formation of episodic memories in the real world. NeuroImage 143, 256–266 (2016).
51. Howard, M. W. & Kahana, M. J. A Distributed Representation of Temporal Context. Journal of Mathematical Psychology 46, 269–299 (2002).
52. Howard, M. W. & Kahana, M. J. When Does Semantic Similarity Help Episodic Retrieval? Journal of Memory and Language 46, 85–98 (2002).
53. Staudigl, T., Vollmar, C., Noachtar, S. & Hanslmayr, S. Temporal-pattern similarity analysis reveals the beneficial and detrimental effects of context reinstatement on human memory. J Neurosci 35, 5373–5384 (2015).
54. Staudigl, T. & Hanslmayr, S. Reactivation of neural patterns during memory reinstatement supports encoding specificity. Cogn Neurosci 10, 175–185 (2019).
55. Manning, J. R., Polyn, S. M., Baltuch, G. H., Litt, B. & Kahana, M. J. Oscillatory patterns in temporal lobe reveal context reinstatement during memory search. Proceedings of the National Academy of Sciences 108, 12893–12897 (2011).
56. Miller, J. F. et al. Neural activity in human hippocampal formation reveals the spatial context of retrieved memories. Science 342, 1111–1114 (2013).
57. Schechtman, E., Heilberg, J. & Paller, K. A. Made together, replayed together: Context reinstatement during sleep guides memory consolidation. 2022.03.28.486140 Preprint at https://doi.org/10.1101/2022.03.28.486140 (2022).
58. Ngo, H.-V. V. & Staresina, B. P. Shaping overnight consolidation via slow-oscillation closed-loop targeted memory reactivation. Proc Natl Acad Sci U S A 119, e2123428119 (2022).
59. Helfrich, R. F., Mander, B. A., Jagust, W. J., Knight, R. T. & Walker, M. P. Old Brains Come Uncoupled in Sleep: Slow Wave-Spindle Synchrony, Brain Atrophy, and Forgetting. Neuron 97, 221-230.e4 (2018).
60. Buysse, D. J., Reynolds, C. F., Monk, T. H., Berman, S. R. & Kupfer, D. J. The Pittsburgh sleep quality index: A new instrument for psychiatric practice and research. Psychiatry Research 28, 193–213 (1989).
61. Horne, J. A. & Ostberg, O. A self-assessment questionnaire to determine morningness-eveningness in human circadian rhythms. Int J Chronobiol 4, 97–110 (1976).

62. Konkle, T., Brady, T. F., Alvarez, G. A. & Oliva, A. Conceptual distinctiveness supports detailed visual long-term memory for real-world objects. J Exp Psychol Gen 139, 558–578 (2010).
63. Brainard, D. H. The Psychophysics Toolbox. Spat Vis 10, 433–436 (1997).
64. Iber, C., Ancoli-Israel, S., Chesson, A. L. & Quan, S. F. The AASM Manual for the Scoring of Sleep and Associated Events: Rules, Terminology, and Technical Specification. (American Academy of Sleep Medicine, 2007). doi:10.1007/978-3-7985-1852-0.
65. Oostenveld, R., Fries, P., Maris, E. & Schoffelen, J.-M. FieldTrip: Open source software for advanced analysis of MEG, EEG, and invasive electrophysiological data. Comput Intell Neurosci 2011, 156869 (2011).
66. Davachi, L. Item, context and relational episodic encoding in humans. Curr Opin Neurobiol 16, 693–700 (2006).
67. Gross, J. et al. Dynamic imaging of coherent sources: Studying neural interactions in the human brain. Proc. Natl. Acad. Sci. U.S.A. 98, 694–699 (2001).
68. Oostenveld, R., Stegeman, D. F., Praamstra, P. & van Oosterom, A. Brain symmetry and topographic analysis of lateralized event-related potentials. Clinical Neurophysiology 114, 1194–1202 (2003).
69. Tzourio-Mazoyer, N. et al. Automated anatomical labeling of activations in SPM using a macroscopic anatomical parcellation of the MNI MRI single-subject brain. Neuroimage 15, 273–289 (2002).
70. Treder, M. S. MVPA-Light: A Classification and Regression Toolbox for Multi-Dimensional Data. Frontiers in Neuroscience 14, (2020).
71. Jackson, J. E. A user's guide to principal components. (Wiley-Interscience, 2003).
72. Lemm, S., Blankertz, B., Dickhaus, T. & Müller, K.-R. Introduction to machine learning for brain imaging. Neuroimage 56, 387–399 (2011).
73. King, J.-R. & Dehaene, S. Characterizing the dynamics of mental representations: the temporal generalization method. Trends Cogn Sci 18, 203–210 (2014).
74. Kriegeskorte, N. Pattern-information analysis: from stimulus decoding to computational-model testing. Neuroimage 56, 411–421 (2011).
75. Zhang, H., Fell, J. & Axmacher, N. Electrophysiological mechanisms of human memory consolidation. Nat Commun 9, 4103 (2018).
76. Griffiths, B.G., Schreiner, T, Schaefer, J., Vollmar, C., Kaufmann, E., Quach, S., Remi, J., Noachtar, S., Staudigl, T. Electrophysiological signatures of veridical head direction in humans. BiorXiv (2023)

Acknowledgements

This work was supported by the European Research Council (https://erc. europa.eu/, Starting Grant 802681 awarded to TSt). We are indebted to all patients and participants who volunteered to participate in this study. We thank the staff and physicians at the Epilepsy Center, Department of Neurology, Ludwig Maximilians University, Munich for assistance.

Competing interests

The authors declare no competing interests.

Supplementary Information

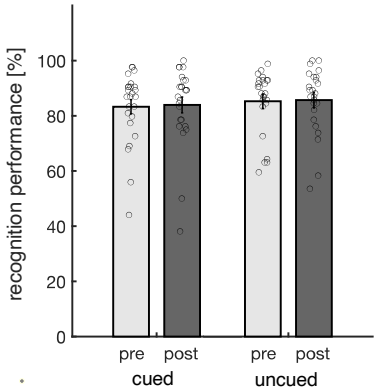

Supplementary Fig. 1. Recognition memory performance (EEG study). Behavioral results for both experimental sessions pre- (light gray) and post-sleep (dark gray), separated into cued and uncued trials. Bar graphs show mean (±SEM) percentage of correctly recognized images ('hits'). Dots indicate individual memory performance of participants (N = 25). There was neither a significant main effect of test time ($F_{1,24}$ = 0.29; p =0.59), nor a significant interaction between test-time and cueing ($F_{1,24}$ = 0.08; p =0.77).

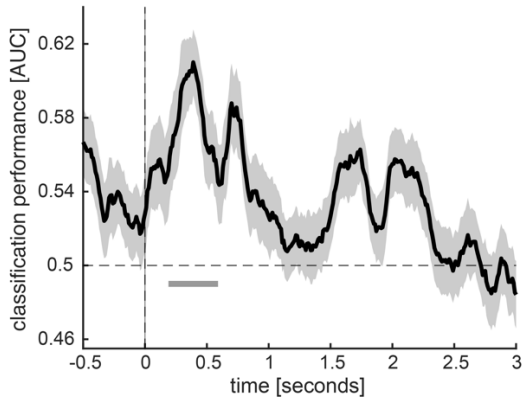

Supplementary Fig. 2. Classification of later not cued head-orientations during retrieval. Later not cued head orientations (left vs. right) could be reliably decoded (above chance) from the retrieval data between 190 and 590 ms after the onset of the associate prompt (the black solid line indicates decoding performance (±SEM)). The horizontal dashed line indicates chance level performance (i.e., 0.5). The vertical solid line indicates the onset of associative memory test trials (time = 0). The lower horizontal gray line shows the temporal extent of significant decoding results as derived from a dependent-samples t-test (two-sided, p < 0.006, cluster corrected across time).

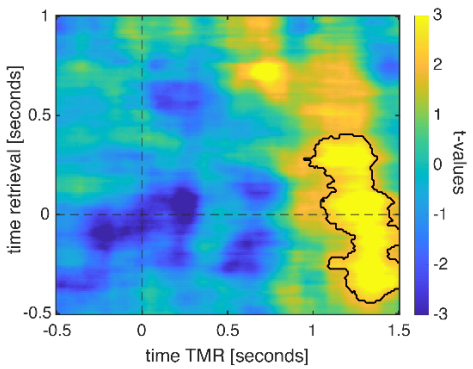

Supplementary Fig. 3. Classification using TMR trials exhibiting increased levels of activity in the SO-spindle range. Learning-related brain patterns (left vs. right head-orientations) were reliably decodable during 'high power' TMR trials (contour lines indicate the extent of the significant cluster, p = 0.005 corrected; color range (blue to yellow) represents t values against chance level performance (i.e., 0.5)).

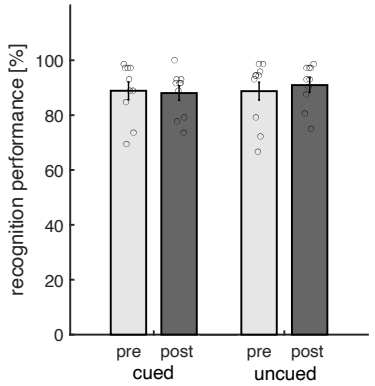

Supplementary Fig. 4. Recognition memory performance (iEEG study). Behavioral results for both experimental sessions pre- (light gray) and post-sleep (dark gray), separated into cued and uncued trials. Bar graphs show mean (±SEM) percentage of correctly recognized images ('hits'). Dots indicate individual memory performance of participants (N = 10). There was neither a significant main effect of test time ($F_{1,9}$ = 0.06; p =0.08); nor a significant interaction between test-time and cueing ($F_{1,9}$ = 2.25; p =0.16).

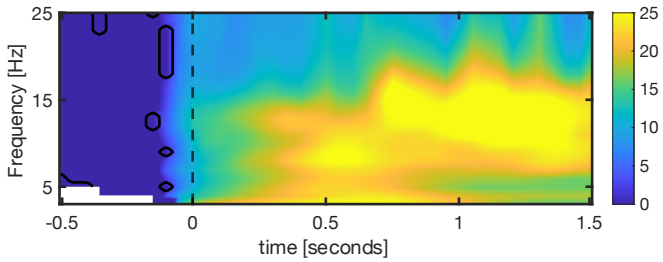

Supplementary Fig. 5. Time–frequency representation difference map of high and low power trials. Oscillatory power was significantly higher for all time and frequency bins starting around cue onset for high power trials. Note the low frequency activity around 500 ms and subsequent spindle activity standing out (12-16Hz; p < 0.00001, corrected for multiple comparisons across time and frequency).

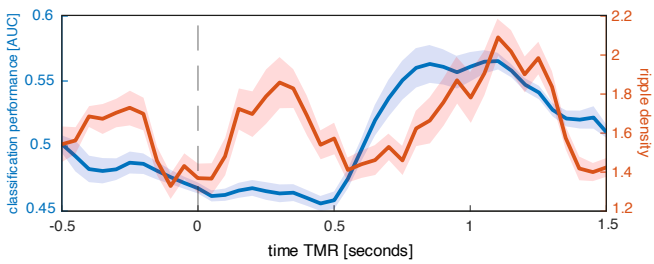

Supplementary Fig. 6. Time course of ripple density and reactivation signal. Blue: Classification output averaged across the relevant retrieval time [-180 to 100 ms]. Red: Patient-averaged ripple density across time.

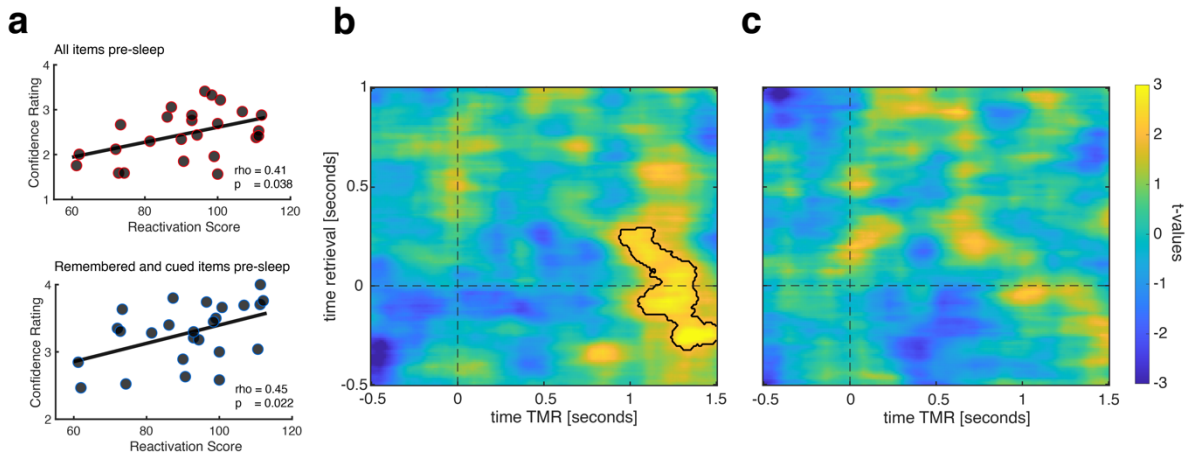

d

	Pre	Post	Pre-rem	Post-rem	Pre high conf. rem	Post high conf. rem
Confidence	2.5 ± 0.5	2.3 ± 0.6	3.2 ± 0.3	3.3 ± 0.2	54.39 ± 3.97 %	55.53 ± 3.99 %

Supplementary Fig.7. Relationship of confidence ratings and memory reactivation. In each retrieval trial participants indicated how confident they were with their head orientation decision (scale from 0 corresponding to very uncertain to 4, very certain). (a) Participants' average confidence ratings across all trials correlated positively with the behavioral impact of TMR (i.e., reactivation score: relative difference from pre- to post- sleep for cued items - relative difference from pre- to post- sleep for uncued items * 100)/ pre-sleep remembered items; rho = 0.41; p = 0.038). Likewise, participants' average confidence ratings across all remembered and cued trial correlated positively with the behavioral impact of TMR (i.e., reactivation score: relative difference from pre- to post- sleep for cued items - relative difference from pre- to post- sleep for uncued items * 100)/ pre-sleep remembered items; rho = 0.41; p = 0.038). These results suggest that highly confident participants rather benefitted from TMR, while less confident participants exhibited a detrimental effect of TMR. (b) Classification using only high confidence trials (confidence rating = 4) as training data. Learning-related brain patterns (left vs. right head-orientations) were reliably decodable when the decoder was trained on high confidence trials (contour lines indicate the extent of the significant cluster, p = 0.025 corrected; color range (blue to yellow) represents t values against chance level performance (i.e., 0.5)). (c) Classification using lower confidence trials (confidence rating < 4) as training data. Learning-related brain patterns (left vs. right head-orientations) were not decodable when the decoder was trained on lower confidence trials (p = 0.96 corrected; color range (blue to yellow) represents t values against chance level performance (i.e., 0.5)). (d) Descriptives of confidence ratings: Means and SEM of confidence ratings of all pre-sleep trials [Pre], all post sleep trials [Post], all remembered pre-sleep trials [Pre-rem] and all remembered post sleep trials [Post-rem]. Percentage of high confidence trials of all remembered trials in the pre-sleep memory test [Pre high conf. rem] and percentage of high confidence trials of all remembered trials in the post-sleep memory test [Post high conf. rem].

	N1	N2	SWS	REM	WASO	TST [min]
Sleep stage [%]	4.1 ± 0.5	46.8 ± 1.4	22.6 ± 1.0	21.0 ± 1.2	0.04 ± 0.01	421.4 ± 9.7

Supplementary Table 1. Sleep characteristics EEG study. Data are means ± s.e.m. N1, N2: NREM sleep stages N1 & N2, SWS: slow-wave sleep, REM: rapid eye movement sleep, WASO: wake after sleep onset.

	N1	N2	SWS	REM	WASO	TST [min]
Sleep stage [%]	4.1 ± 0.9	44.9 ± 2.7	20.6 ± 2.5	23.1 ± 2.0	5.2 ± 1.7	480.3 ± 31.4

Supplementary Table 2. Sleep characteristics iEEG study. Data are means ± s.e.m. N1, N2: NREM sleep stages N1 & N2, SWS: slow-wave sleep, REM: rapid eye movement sleep, WASO: wake after sleep onset.